EFFECTS OF LIVER-SPECIFIC ACSL4 (LONG-CHAIN ACYL-COENZYME A SYNTHETASE 4) DELETION IN LIVER LIPID METABOLISM

Guo Hu

A thesis submitted to the faculty of the University of North Carolina at Chapel Hill in partial fulfillment of the requirements for the degree of Master of Science in the Department of Nutrition (Nutritional Biochemistry) in the Gillings School of Global Public Health.

Chapel Hill
2014

Approved by,

Rosalind Coleman

Eric L. Klett

Melinda Beck

© 2014
Guo Hu
ALL RIGHTS RESERVED

ABSTRACT

Guo Hu: Effects of liver-specific ACSL4 (long-chain acyl-Coenzyme A synthetase 4) deletion in liver lipid metabolism
(Under the direction of Dr. Rosalind Coleman)

Long-chain Acyl-CoA synthetases (ACSLs) are a family of enzymes that catalyze the thioesterification of free fatty acid to fatty acyl-CoA. One member of this family, ACSL4 has been found to be overexpressed 3-fold in patients with non-alcoholic fatty liver disease (NAFLD) though the role of ACSL4 in the pathogenesis of NAFLD is unknown. We hypothesized that the absence of ACSL4 would prevent NAFLD development. In order to test our hypothesis we developed a murine liver-specific Acsl4 knockout, fed them a high fat diet (HFD), and determined if they were protected from the development of fatty liver. Despite 20 weeks of a 45% HFD, no difference was observed in weight gain, insulin sensitivity, ACSL activity, liver triacylglycerol content, liver histology, or serum lipid metabolites between control and Acsl4 liver specific knockout animals. These results indicated that Acsl4 liver-specific KO mice were not protected from developing a fatty liver.

To my grandma, mom and dad, and all my friends

Sincerely thank for your support, assistance, and solid belief on me

ACKNOWLEDGEMENTS

My deepest gratitude goes first and foremost to Dr. Rosalind Coleman, my supervisor and mentor, for her constant encouragement and guidance which led me to accomplish my two year study abroad. Her commitment and attitude to science inspired me to devote myself to research and shaped my future career. I am highly indebted to my committee members, Dr. Eric Klett and Dr. Melinda Beck, who gave me immense help and advice on my project with their knowledge and time. Also, I would like to express my appreciation to other previous and current members in Dr. Coleman's lab, particularly Chongben Zhang, Trisha Grevengoed, Daniel Cooper, and Amanda Crunk for their endless patience with my requests for advice. It is my duty to record special gratitude to our Nutrition department for this valued opportunity of two-year education in science. Finally, I would love to thank my parents and friends who never lose faith in me for their unwavering support and warmest encouragement.

TABLE OF CONTENTS

LIST OF TABLES

LIST OF FIGURES

LIST OF ABBREVIATIONS

AA	Arachidonic acid
AAC	Area above the curve
ACC	Acetyl-CoA carboxylase
ACSL	Long-chain acyl-CoA synthetase
ACSL4 $^{L-/-}$	Long-chain acyl-CoA synthetase 4 liver-specific knockout
ACSs	Acyl-CoA synthetases
ApoC	Apolipoprotein C
AUC	Area under the curve
CE	Cholesterol esters
CLD	Cytoplasmic lipid droplets
CoA	Coenzyme-A
ChREBP	Carbohydrate response element binding protein
DGAT	Diacylglycerol acyltransferase
FAS	Fatty acid synthetases
FA	Fatty acid
FFA	Free fatty acid
GPAT	Glycerophosphate acyltransferase
HFD	High fat diet
I.P.	Intraperitoneal injection
IR	Insulin resistance
ITT	Insulin tolerance test
KO	Knockout

LPL	Lipoprotein lipase
Lyso-PA	Lysophosphatidic acid
MR	Mental retardation
MTP	Microsomal triglyceride transfer protein
NAFLD	Non-alcoholic fatty liver disease
NEFA	Non-esterified fatty acid
OGTT	Oral glucose tolerance test
ORO	Oil red O
PA	Phosphatidic acid
PC	Phosphatidylcholine
PE	Phosphatidylethanolamine
PG	Phosphatidylglycerol
PI	Phosphatidylinositol
PL	Phospholipid
PPAR-γ	Peroxisome proliferator activated receptor-γ
PUFA	Polyunsaturated fatty acids
SREBP-1c	Sterol regulatory element binding protein-1c
TAG	Triglyceride
VLDL	Very low-density lipoprotein
WT	Wild-type

Chapter I. Introduction

1.1 Hepatic lipid metabolism

The liver is one of the most metabolically active organs in the body and acts as the core lipid metabolic factory via fatty acid (FA) synthesis, complex lipid formation, very low-density lipoprotein (VLDL) production and secretion, and fatty acid oxidation. Each of these metabolic pathways involves numerous enzymes that interact with one another and are regulated through different genetic, hormonal, and nutritional conditions. Acyl-CoA synthetase 4 (*ACSL4*) is – one of five ACSL isoforms – that catalyzes the initial step of free fatty acid activation. Each isoform appears to have slightly different functions and it has not been established as to how and where those activated FAs might be used. My goal was to investigate the function of ACSL4 in liver and determine its role in hepatic lipid metabolism.

Lipid metabolism first begins with the digestion and absorption of fat from the diet. Triglyceride digestion is initiated by lingual lipases which are secreted by the tongue and is further processed in the stomach [1]. The stomach is the primary site for emulsification of fat-soluble vitamins and dietary fat [1]. The emulsification process continues as the micelle moves towards the duodenum. The pancreas secretes multiple enzymes, such as lipases, which hydrolyze dietary complex lipids with the help of bile and bile salts in the intestine. FFA and 2-monoacylglycerol, which are disassembled from dietary triacylglycerol (TAG), are taken up by intestinal cells through protein-mediated, as well as protein- independent, processes [1]. Cholesterol esters (CE), phospholipids (PL), and

re-synthesized TAG are exported through chylomicrons from intestinal cells into the circulation. Lipoprotein lipase (LPL) hydrolyzes the TAG from chylomicrons for the use of peripheral tissues. The remnant chylomicrons, along with VLDL remnants, are taken up by liver through LDL-receptors. Within hepatocytes, lipid components, released from remnants, enter different metabolic pathways. Long-chain fatty acids are covalently bound and activated by ACSL and are partitioned into different metabolic pathways [2].

Activated FAs that enter synthetic pathways can be stored in cytoplasmic lipid droplets (CLD) or incorporated into complex lipids. The lipid formation pathway depends on whole body energy status and nutrient requirements. Synthetic lipid mechanisms in liver include *de novo* lipogenesis, TAG, and phospholipid synthesis. Acetyl-CoA carboxylase (ACC) catalyzes the conversion of acetyl-CoA to malonyl-CoA and is one of the rate-limiting enzymes of *de novo* lipogenesis. ACC activity is inhibited under energy-insufficient state. Elongation of malonyl-CoA is catalyzed by fatty acid synthetase (FAS), which is expressed in both liver and adipose tissues, by adding acetyl-CoA in each round until the formation of palmitic acid. The rate of *de novo* lipogenesis is highly regulated by hormones such as insulin and glucagon. Insulin and glucagon are raised during fed and fasting states, respectively. Furthermore, carbohydrate and specific fatty acid content such as n-3 polyunsaturated fatty acid in different diets can alter the expression of lipogenic genes by activating transcription factors such as SREBP-1c, ChREBP, and PPAR-γ.

TAG synthesis is initiated by FA activation catalyzed by ACSLs. The following esterification steps are catalyzed by glycerophosphate acyltransferase (GPAT), lysophosphatidate acyltransferase and diacylglycerol acyltransferase (DGAT) which lead to the formation of lysophosphatidic acid (lyso-PA), diacylglycerol (DAG) and triacylglycerol

(TAG), respectively. Phospholipid formation is processed by using intermediates from TAG synthesis pathway. Phosphatidic acid (PA) derived from lyso-PA can be used as a backbone for phospholipid formation through two different mechanisms. One pathway involves hydrolyzing the phosphate group from PA to form DAG, with DAG serving as a precursor for phosphatidylethanolamine (PE) and phosphatidylcholine (PC). The other pathway accounts for the major phosphatidylinositol (PI) and phosphatidylglycerol (PG) production by catalyzing CDP-DAG formation from PA. The fate of newly formed TAG and phospholipids in liver is controlled by whole body energy states, either to be accumulated into CLD or output by VLDL.

Unlike adipose tissue, the major site for lipid storage, the liver serves as a distribution center for the exports of TAG, phospholipids, and CE by secreting these lipids into VLDL particles for delivery into the circulation for utilization in the peripheral tissues. Hepatic levels of lipid and ApoB100 are the two main components which directly affect VLDL assembly. Increased plasma non-esterified fatty acid (NEFA) induces VLDL production and hepatic esterification [3] which are exacerbated in an insulin-resistant state [4, 5]. Insulin decreases VLDL production by increasing ApoB100 protein degradation [6] and inhibiting microsomal triglyceride transfer protein (MTP) expression, a protein is required for lipoprotein assembly [7].

The degradative pathway of activated fatty acids metabolism is β-oxidation. This pathway takes place in the mitochondria, resulting in formation of acetyl-CoA from acyl-CoA. These acetyl-CoAs can be used as energy production through tricarboxylic acid cycle (TCA) and electron transport chain. Increased NADH and FADH, generated by the oxidation pathway and TCA cycle, donate electrons to the electron transport chain to drive ATP

synthesis for energy production. The energy that is yielded from fatty acid oxidation is approximately 9 Kcal of energy per gram of fatty acid – more than twice the amount of what is produced from a gram of carbohydrates during glycolysis of glucose. Under prolonged fasting or aerobic exercise, both of which require an increased energy supply, the main energy utilization shifts from glucose to FA.

1.2 Role of ACS isoforms in lipid metabolism

Long-chaine Acyl-Coenzyme A (acyl-CoA) synthetases (ACSLs) are a group of enzymes that play an essential role in lipid metabolism including *de novo* lipid synthesis, fatty acid degradation, and membrane remodeling. Though all ACSL isoforms share the same capacity for thioesterification of free fatty acid to fatty acyl-CoA, the substrate specificity, subcellular location, and potential impact on downstream metabolic pathways differ amongst each of the ACSLs isoforms. Although structurally similar to one another, the five ACSL members can be grouped based upon their difference of sequence homology and gene structure into two sub-groups: ACSL1/ACSL5/ACSL6 and ACSL3/ACSL4 [8]. Most of the ACSL isoforms are membrane-associated, but ACSL4 variant 1 is found in the cytoplasm [9]. Though enzyme activity can be measured in multiple ways, accurate assessment of the activity of each isoform is still a major challenge because inhibitors of ACSL are the non-specificity. For example, in the mitochondrial membrane, triacsin C can selectively inhibit the activity of ACSL1, ACSL3, and ACSL4 without affecting ACSL5 or 6 [10, 11]. The activity of ACSL4 is selectively and directly diminished by the use of thiazolidinediones in a dose-dependent manner [12]; thiazolidinediones also decreases triglyceride production and circulating free fatty acids by activating PPAR-γ [13]. Therefore,

how their distinct structure determines specific functions of each isoform and their locations and activities is still not clear [14]. Due to the diversity of tissue distribution and subcellular localization, we assume that each ACSL isoform plays a unique role in lipid metabolism. In our study, by using the ACSL4 $^{L-/-}$ mouse model, we aimed to investigate the role of ACSL4 in hepatic lipid metabolism.

1.3 *ACSL4* gene structure and expression

Long-chain acyl-CoA synthetase 4 (ACSL4) is a member of the ACS family that is encoded by the *ACSL4* gene found on the X-chromosome [15]. The ACSL4 protein contains 711 amino acids and exists in brain and steroidogenic tissues [15]. Two identified protein domains, AMP-dependent synthetase/ligase and a conserved site with AMP-binding, form the enzyme structure [16-19]. On the *ACSL4*, various sites located on *ACSL4* promoter are available for different regulatory transcription factors such as Egr-3 [20], SRF [21], AP-2 gamma [22]. These transcriptional regulators participate in the regulation of *ACSL4* genes expression in different situations such as embryo development [21], circadian rhythm [20], and muscle development [22]. Different splice variants of the *ACSL4* gene can produce two possible ACSL4 isoforms. Variant 1 is the truncated isoform of 75KDa molecular weight and predicted by PSORT to localize within the cytoplasm [23, 24]. On the other hand, the longer variant 2 isoform contains an additional 41-amino acids at the N-terminus [15, 23] with a total molecular weight of ~79KDa [15]. The additional 41-amino acids in variant 2 are highly hydrophobic , targeting this variant to the membranes [24] both the outer nuclear membrane and endoplasmic reticulum (ER) membrane [24] of the brain [24, 25].

1.4 ACSL4 location and substrate preference

Each ACS isoform is likely to have specific fatty acid (FA) preference and can have differing tissue distributions. Compared with other isoforms, ACSL4 has a high affinity for polyunsaturated fatty acids (PUFA) including arachidonic acid (AA) (20:4) as substrates [26], and it showed lower affinity for mono-, di-, and tri-saturated FAs [26] among the C8–C22 saturated fatty acids and C14–C22 unsaturated fatty acids that were tested [26]. This result was supported by kinetic studies with a purified recombinant Acsl4 from *Escherichia coli* that had been engineered to overproduce rat ACSL4 [26], which has 91% similarity by comparison of nucleic acids or a 97% identity for amino acids to human ACSL4 [26, 27]. The localization of ACSL4 is distinct from other isoforms as well. Specific regions in the brain, which includes the cerebellum and the hippocampus, have higher ACSL4 expression compared to other regions of the brain [26]. The mRNA expression of *ACSL4* is also detected in steroidogenic tissues including adrenal gland, ovary, and testes [26]. The ACSL4 is one of the ACSL isoforms present in human arterial smooth muscle cells (SMCs) in addition to ACSL1, ACSL3, and ACSL5 [12].

With PUFAs, specifically arachidonic acid the preferred substrate of ACSL4, it is likely that ACSL4 plays a significant role in eicosanoid metabolism. Meanwhile, oxygenated AA generates inflammatory products which modulate and mediate the inflammatory response. To prevent excessive synthesis of eicosanoids, which can stimulate inflammation and immune reaction, free arachidonate is converted to arachidonoyl-CoA and re-esterified into phospholipids as the safe and storage form [28-30]. In general, phospholipid is formed by an esterified saturated fatty acid at the sn-1 position of the glycerol backbone, an unsaturated fatty acid at the sn-2 position, and a head group linked by a phosphate residue at

the sn-3 position. AA is normally added at the sn-2 position. Data from rat liver showed amongst phospholipid species, 36.3% of PI contains AA [31]. AA is also the most abundant unsaturated fatty acid in PE and PC (about 23%) [32]. Upon being absorbed from diet or released from phospholipids or other esters by phospholipase A_2 (PLA_2) [33], AA can be further metabolized into different eicosanoids via either the cycloxygenase (COX), lipoxygenase (LOX) or cytochrome P450 monooxygenase pathways [34, 35]. The major product of the COX pathway is prostaglandins including prostaglandin G_2 (PGG_2), PGH_2, and PGE_2 [34]. Leukotrienes and hydroxyeicosatetraenoic acids (HETEs) are made by activated LOXs and produce their biological effects by interacting with correspondent cognate G protein-coupled receptors [34]. Hydroperoxyeicosatetraenoic acids (HPETEs), epoxyeicosatrienoic acids (EETs) and HETEs are synthesized from AA by p450 pathway and have major effects in the regulation of ion transport [35, 36]. Expression of these eicosanoids is tightly controlled by the activity and expression of key enzymes in each pathway [35]. Cholesterol ester hydrolase, a key enzyme in steroidogenesis, releases AA from cholesterol esters, which is the key regulated enzyme in steroidogenesis [37]. As an omega-6 FA with multiple double bonds which are easily oxidized, arachidonic acid exerts its influence in multiple ways within vascular cells. This characteristic is considered a contributor of atherosclerotic disease in humans due to its effects on reduction of unstable atherosclerotic plaques [38]. Knocking down the *Acsl4* in INS 832/13 cells, EETs in the media was increased after incubation with 17 mM glucose, and EETs in cell membrane was reduced [39]. Glucose-stimulated insulin secretion in those cells was reduced by exogenous EETs. The result indicated in pancreatic beta-cells, ACSL4 catalyzed EET-CoAs activation by thioesterify the unesterified EETs. Further, this reaction positively modulates glucose-

stimulated insulin secretion [39]. However, due to lack knowledge of ACSL4 function in liver, whether hepatic EETs will be affect by ACSL4 expression and further alter the hepatic lipid metabolism is still unknown.

1.5 Abnormality of *ACSL4* in human disease

A large sequence deletion around the area of the *ACSL4* results in a constellation of diseases including elliptocytosis, Alport syndrome, and mental retardation (MR) [15]. Amongst these diseases, only mental retardation is associated with deficiency of ACSL4 [15]. Given that ACSL4 expression is the highest in the hippocampus and the cerebellum [26] indicates this enzyme might have an essential role in normal brain function. To investigate ACSL4 function during brain development, investigators showed that there was higher expression of ACSL4 in the brain of newborn mouse compared to the brains of adult mouse [40]. Alport syndrome, caused by the deletion of the entire COL4A5 gene which contains *ACSL4* encoding sequence, leads to a high risk of renal failure among males by adult age [15]. This X-linked illness was potentially caused by an *ACSL4* abnormality that alters neural lipid metabolism [15].

1.6 Hepatic lipid metabolism and NAFLD with ACSL4

Non-alcoholic fatty liver disease begins with benign fat accumulation and exacerbates by excessive fatty infiltration and inflammation to overt cirrhosis. Chronically increased fat accumulation in the liver impairs the normal hepatic response to insulin, which disturbs the production of glucose [41] and VLDL secretion [42, 43]. Insulin resistance impairs the regulation of gluconeogenesis in the liver, so that insulin resistance increases hepatic glucose

output under an unnecessary condition. Along with impaired glucose uptake in peripheral tissues, these abnormal conditions may lead to hyperglycemia [44], hypertriglyceridemia, hyperinsulinemia, and a low HDL-cholesterol concentration in circulation [43]. Non-alcoholic fatty liver disease (NAFLD) is strongly associated with metabolic syndrome such as obesity and insulin resistance, and it is identified when the hepatic fat content is above 5% of its total weight in the absence of other causes of steatosis [45]. NAFLD includes multiple aspects of liver dysfunctions such as simple steatohepatitis (nonalcoholic fatty liver disease [NAFL]) and cirrhosis, and can be a precursor to type 2 diabetes, cardiovascular disease, and liver failure [46]. In hepatic lipid metabolism, acyl- CoA synthetases are essential in the initial step of acyl-CoA formation from free long-chain fatty acids. ACSL4 has been found up-regulated ranged from 2.3 to 27.5 folds in hepatocellular carcinoma compared to non-cancerous tissues [47]. In in vitro studies within breast cancer cell lines, ACSL4 promotes MCF-7 cells proliferation about 1.5- to 2-fold [48, 49]. Meanwhile, in colon cancer the overexpression of Acsl4 mRNA has been found ranged between 2.4 to 54.5 fold and ranged 2.4 to 64 fold of increment of ACSL4 protein expression [50]. Studies using CLOCK-deficient mice suggest that Acsl4 plays a role in the development of hepatosteatosis as these mice had reduced Acsl4 and Fabp1 expression leading to reduced steatosis on a HFD [51]. CLOCK transcription factor, which is encoded by the clock gene, participates in regulation of body temperature and metabolic regulations [51]. This result suggests that *Acsl4* expression or protein function may alter lipid metabolism which is involved in circadian control [51]. In human studies, ACSL4 also contributes to the development of human hepatocellular carcinoma and adenocarcinoma [47, 52, 53]. Among 302 Finnish subjects after adjusting for BMI, sex, and age, researchers first saw polymorphisms in *ACSL4* that

were significantly related to liver fat content [54]. Higher hepatic lipid content of NAFLD patients, accompanied by an increased insulin concentration and obesity, was observed among subjects with high expression of a rare allele of *ACSL4* rs7887981 [54]. Based upon these numerous associations between NAFLD and Acsl4 overexpression, we aimed to determine whether ACSL4 expression is the cause or consequence of NAFLD and whether ACSL4 deletion would prevent hepatic steatosis in diet-induced obesity. We hypothesize that deletion of ACSL4 will prevent diet-induced non-alcoholic fatty liver disease.

Chapter II Development of ACSL4 liver specific knockout mice

ACSL4 deficiency was first indicated in 1% of X-linked mental retardation from human studies [15]. Overexpression of ACSL4 has been found in different cancer studies. In recent years, ACSL4 was also implicated by the fact that ACSL4 mRNA was 2.8-fold higher in the liver of NAFLD patients [54]. However, the function of ACSL4 in lipid metabolism and how ACSL4 uniquely impact hepatic lipid homeostasis are not fully understood. To investigate the function of ACSL4, we developed a strain of liver-specific ACSL4 knockout mice in C57BJ/6 background by using loxP-Cre strategy.

2.1 Generation of ACSL4 liver-specific knockout mice (*Acsl4* $^{L-/-}$)

The *Acsl4* gene is located on X-chromosome Xq22.3-q23 with a total 104,054 base pairs and contains at least 17 exons [55]. This gene encodes the ACSL4 protein which has a molecular weight of 79kDa. We have developed an *Acsl4*$^{floxed/floxed}$ mouse with gene-targeting vector which is designed to produce a floxed *Acsl4* gene. *LoxP* sites were inserted outside exons 3 and 4 of the *Acsl4* gene. Insertion of *LoxP* sites should not alter the expression of ACSL4, but only allow Cre to cut at these sites to remove the DNA between the sites. For positive screening of *LoxP* insertion, neomycin phosphotransferase (neo) was included in the construction of the vector. A map of the engineered allele with the excision of exons 3 and 4 shows the gene structure (**Figure 1A**). Stem cells with 129S1/SvlmJ background which contained positive gene construction were microinjected into blastocysts

with C57BL/6 background to produce transmitting chimeras. *Flpo* recombinase expressed in transgenic mice was used to excise neo sequence from the targeted allele. To purify the genetic background, heterozygous ACSL4 floxed female mice ($ACSL4^{+/-}$) were back-crossed 10-times to C57BL/6 mice. The $ACSL4^{+/-}$female mice were mated with albumin promoter-Cre transgenic male mice from Jackson lab (JAX Mice Database - 003574 B6.Cg-Tg(Alb-cre)21Mgn/J), in which the Cre recombinase is uniquely expressed in liver [56]. Because *Acsl4* is X-linked, we used male knockout mice for our experiments ($ACSL4^{L-/-}$) and 3 different groups of littermate controls at first ($ACSL4^{+/+}$-Cre+, $ACSL4^{+/+}$- Cre^{-}, and $ACSL4^{-/-}$ - Cre^{-}) (**Figure 1B**). Because the founder Alb-Cre transgenic mice were heterozygous, ideally the offspring will have 50% chance to inherit Cre gene. Using Cre-specific primer, we determined the existence of Cre. The genotype was confirmed with A/B primers which were designed to detect *LoxP* insertion (**Table 1A**) by using DNA extracted from tail samples **(Table 1A**). Further ensuring deletion of the *Acsl4* in the liver, A/C primers are used in PCR solution by using DNA extracted from liver. Sizes of PCR products by using A/B or A/C primers differed from each other (**Table 1B**). PCR products from liver samples showed knockout genotype with a bright band around 283bp (**Figure 1B**), whereas that band is absent when DNA was extracted from littermate controls (**Figure 1B**).

2.2 Mating strategies of ACSL4 LoxP-Cre mice

By crossing an $ACSL4^{+/-}$ female with a heterozygous Alb-Cre male, we obtained $ACSL4^{L-/-}$ male mice with ideal chance of 12.5%. To increase the number of $ACSL4^{L-/-}$ mice produced, we set up new mating cages by developing $ACSL4^{floxed/floxed}$ females which

we interbred with heterozygous Alb-Cre male mice. The new strategy increased the predictedrate of production of male knockout mice to 25% (**Table 2**).

2.3 Liver *Acsl4* mRNA level and protein expression in liver specific knockout mice

To determine whether deletion of exons 3 and 4 eliminated *Acsl4* expression in the liver of knockout mice, total RNA was extracted from ACSL4 $^{L-/-}$ livers and littermate control livers (Qiagen RNeasy Mini kit). cDNA was made by reverse transcription (Applied Biosystems). The mRNA level of each ACSL isoform was detected with forward primers and reverse primers (**Figure 2**). *Acsl4* mRNA expression was highly reduced in liver-specific knockout mice compared with wild-type littermates. Absence of *Acsl4* did not alter expression of other ACSL isoforms.

Mouse peptide antibody against mouse ACSL4 (ACSL4 antibody, supplied by Dr. S. Prescott – University of Utah) was used to detect ACSL4 protein expression. We detected a ~75kDa band in liver from littermates control mice, but ACSL4 protein was absent in liver from ACSL4 $^{L-/-}$ mice. ACSL4 protein was still expressed in kidney and gonadal adipose tissue from both genotypes, which confirms the liver-specific ACSL4 deletion. (**Figure 2B**)

Chapter III Materials and Methods

3.1 Animal model and tissue collection

All procedures were reviewed and approved by the Institutional Animal Care and Use Committee (IACUC) of the University of North Carolina at Chapel Hill (Chapel Hill, NC, USA). Mice from the same generation were housed together in a 12-hour light-dark cycle and temperature controlled environment.

Male mice were weaned around 21 days of age with littermates, and were housed together and fed a standard chow diet (Prolab RMH 3000 SP76 chow). At 8 weeks, ACSL4 $^{L-/-}$ mice and their littermates controls were fed a high fat diet (HFD; 45% calories from fat majority from lard), 35% calories from carbohydrate (sucrose and corn starch) Research Diets D12451) or an iso-caloric matched diet (10% calories from fat using lard and soybean oil, 70% from carbohydrate (matched with sucrose but higher in corn starch) Research Diets D12451H) for 20-22 weeks. Weight was recorded weekly. Oral glucose tolerance tests (OGTT) and insulin tolerance tests (ITT) were performed at week 18-19 and week 20-21, respectively. One week after the insulin challenge, mice were sacrificed after a 4 h fast (from 9 am to 1 pm). Plasma was collected from the retro-orbital sinus and mixed with 10 μl 0.5 M EDTA. Liver, unilateral kidney, unilateral gonadal adipose tissue, and unilateral inguinal adipose tissue were weighed, snap-frozen in liquid nitrogen, and stored at -80 ℃.

3.2 Oral glucose tolerant test (OGTT) and insulin tolerant test (ITT)

Oral glucose tolerance tests were performed after a 4 hour fast (from 9 am to 1 pm). Fasting blood glucose level was measured by glucose monitor (Freestyle) before oral gavage (10μl/g) of 20% (w/v) glucose solution (2 g/kg body weight). Blood glucose was measured at 15, 30, 60, 90, and 120 minutes after gavage.

Insulin tolerance tests were performed one week after OGTT. Fasting blood glucose level was measured after a 4 hour fast before intraperitoneal injection (i.p.) of insulin. Insulin solution (0.8 IU/kg) was prepared by diluting the insulin stock (100 IU/ml) with PBS. Glucose solution (20% w/v) was available for rescuing if mice experienced hypoglycemia when blood glucose lower than 20 mg/dL during the experiment. Blood glucose level was measured at 15, 30, 60, and 90 minutes after intraperitoneal injection (10 μl/g).

3.3 Liver histology

Fresh livers were collected from mice after they were anesthetized with 2.5% Avertin i.p. Liver sections were separated from the left lobe and washed with PBS, place in the mold, and covered in embedding medium (Tissue-Tek O.C.T compound) which solidifies under -10 ℃. Sections were stored at -80 ℃. Each frozen slide contained sections from two livers from both genotypes and was prepared by the Histology Research Core Facility.

Slides were stained with oil red O (ORO) to visualize lipid droplets. ORO stock solution was made by 400 ml 99% isopropyl alcohol and 2.5 g ORO powder and stored at

room temperature. Diluted ORO stock was diluted 3:2 (v/v) with water to make THE working solution and filtered before use. Frozen sections first were air-dried for 10 minutes and fixed with 10% formalin solution for 30 minutes. After rinsing with PBS buffer, slides were dipped into ORO working solution for 15 minutes, followed by a wash and then were washed with 60% isopropyl alcohol. A counter stain was done with Mayer's haematoxylin for 1 minute to visualize the nuclei. Slides were washed with running water for 1 minute and mounted in aqueous mounting media (90% glycerol in PBS).

3.4 Liver triglyceride content

TAG content was extracted from liver by a modified Folch method [57, 58]. Snap frozen liver tissues were homogenized in exactly 10x (v/w) ice cold lysis buffer in a plastic microcentrifuge tube. The homogenates were rocked at 4 ℃ for about one hour, then 100 µL liver homogenate of each sample was transferred into tube for TAG content analysis.

After addition of methanol: chloroform (1:2, v/v) liver homogenates were vortexed and incubated at -20 ℃ overnight. 0.24 mL 0.88% KCl was added to break the phases and the mixture was centrifuged at 4 ℃, 1000x g for 15 minutes. The lower chloroform layer was transferred to a new 2mL micro-centrifuge tube and dried under N_2. 0.8mL chloroform was added to the remaining methanol layer, vortexed, and centrifuged again. The second chloroform layer was combined with the previous chloroform extract and dried under N_2.the dried lipid was resuspended by adding 200µl tert-butanol: methanol: Triton X-100 (3:1:1, v/v/v) vortex.

Glycerol that was hydrolyzed from triglyceride in sample reacts with triglyceride reagent. The reaction was visualized by a color change which can be detected at 540 nm after

15 minutes incubation at room temperature. Data was compared to standard glycerol to quantify amount of triglyceride per mg of liver tissue (Sigma).

3.5 Acyl-CoA synthetase activity

Total ACSL activity in liver homogenates was measured with 2, 4, 6 μg liver homogenate at room temperature for 10 minutes with 175 mM Tris (pH7.4), 5 mM dithiothreitol, 8 mM $MgCl_2$, 250 μM CoA, 10 mM ATP, 10 μM EDTA, and 50 μM [1-^{14}C] palmitic acid or 50 μM [^{14}C] arachidonic acid in 500 μM Triton X-100. The total volume was 200 μl [59]. The reaction was stopped by Dole's reagent (isopropanol: heptanes: H_2SO_4; v/v/v =80:20:2) and enzymatic activity was calculated by radioactive counts.

3.6 Serum lipid metabolites

Mice were anesthetized with 2.5% Avertin. The blood was centrifuged for serum collection. The serum was stored at -80 ℃ until use. Colorimetirc kits were used to measure serum TAG (Stanbio), total cholesterol (Wako), and NEFA (Wako).

Chapter IV Investigation of alteration of hepatic lipid metabolism in vitro

After formation by ACS isoforms, acyl-CoAs are distributed to downstream pathways that are disparate due to potentially unique roles of each ACS isoform in lipid metabolism. Deletion of ACSL1 causes a 50% decrease of ACSL activity in liver homogenate [60], pointing to its role as the major ACSL isoform in this tissue. Meanwhile, under lipogenic and oxidative conditions, *ACSL1* mRNA is upregulated [59], which indicates its potential role in both pathways. *ACSL4* mRNA expression in liver of NAFLD human subjects is 2.8-fold higher than in healthy subjects [61] but studies have yet to shed light on ACSL4 function in hepatic liver metabolism. Therefore, developing diet-induced obesity with 45% HFD in ACSL4 $^{L-/-}$ mice provides an opportunity to determine its function.

4.1 Results - Specific activity of total ACSL was identical between genotypes

The absence of ACSL1 in mouse liver resulted in about 50% decrease of ACSL specific activity [60]; therefore, other ACS isoforms must contribute to the remaining the activity. ACSL4 is the only ACSL isoform whose gene expression is altered under NAFLD conditions. We assumed that in our mouse model, by knocking out ACSL4, the total ACSL activity would differ from the activity in littermate control liver. Total ACSL activity was measured with liver homogenates from KO and littermate controls fed a HFD. Arachidonic acid, (**Figure 7A**) considered to be the preferred substrate for ACSL4 [20], and palmitic acid (**Figure 7B**) were used as substrates. With either fatty acid substrate, total ACSL activity

was unchanged in KO liver homogenates compared to control. This result indicates that the deletion of ACSL4 did not alter ACSL specific activity in liver.

4.2 Results - Serum lipid content was unaltered after deletion of ACSL4 in liver

Long-term high fat feeding in mice mimics the Western diet which is considered as the culprit of pandemic obesity and type-2 diabetes in human. Risk of NAFLD is increased by obesity and exacerbated by insulin resistance (IR). Under IR state, restriction of lipolysis in adipose tissue is removed, resulting in an increase in free fatty acids release into the circulation, exacerbating the burden of fatty acid influx into liver [41, 62]. Increased hepatic lipid accumulation may also lead to decreased release of FA from VLDL and reduced fatty acid oxidation [6]. These changes have a great impact on whole body lipid homeostasis. A lard-based HFD contains large amount of saturated fat and cholesterol esters. Increased total serum cholesterol and body weight was reported when B6 mice were fed a 40% HFD, but total triglyceride and blood glucose were unaltered compared to a 17% LFD [63]. To examine if liver-specific ACSL4 deletion in our mouse model would disturb plasma lipid homeostasis, we measured common lipid metabolites in plasma. Total cholesterol, triglyceride, and NEFA values were determined in serum samples from ACSL4 $^{L-/-}$ mice and littermate controls fed a 45% HFD for 20 weeks (**Table 3**). No differences were observed for serum concentrations of total cholesterol, triglyceride, and NEFA between the two genotypes after 20 weeks of 45% HFD-feeding. Compared to LFD controls, HFD significantly increased serum NEFA and cholesterol, but serum triglyceride was decreased after HFD feeding.

Chapter V Physiological siginificance of ACSL4 $^{L-/-}$ mice fed a 45% fat diet

Rodents, one of the major mammalian laboratory models, are widely used for human disease investigation because of their metabolic similarity to humans. To mimic human obesity in murine models, the development of obesity is usually induced by either a genetic mutation or a diet challenge. *Ob/ob* mice, a widely used genetic mutation model for human obesity, develop dramatic weight gain and metabolic disturbance due to the lack of leptin secretion. However, obesity in humans is, in its majority, due to a chronic progression. Apart from a genetic abnormality, consuming high-density caloric food and living a sedentary life act as the major contributing factors to the pandemic proportions of obesity. Therefore, aiming to imitate this gradual onset of obesity, we fed C57BL/6 mice with a 45% HFD. The C57BL/6 mouse is the most popular inbred strain for laboratory use and is normally used as the background strain modeling various human diseases. Compared to other strains, C57BL/6 mice easily develop diet-induced obesity and type 2 diabetes [64]. This susceptibility allows us to investigate the effects of NAFLD derived from diet-induced obesity on transgenic mice challenged by 45% HFD for 20 weeks.

5.1 Results - Diet-induced obesity developed after HFD-feeding.

To explore whether the absence of ACSL4 in liver would disrupt whole body metabolic homeostasis, ACSL4 $^{L-/-}$ male mice and littermate controls were fed a 45% HFD or a 10% LFD matched with sucrose. We were aiming to investigate a diet-induced onset of

NAFLD by using this mouse model to establish a diet-induced obesity. It is reported that body weight gain is not impacted by age of diet initiation (3, 6, or 9 weeks of age) [65]. In another study with 45% HFD feeding, C57BL/6 mice displayed insulin resistance at week 12 [66]. After 21 weeks, these mice showed significant weight gain compared to LFD, along with increased adipose tissue mass and hepatic fat storage [66]. Therefore, in our study mice were weaned after 21 days and housed together. We started the diet for 20 weeks when the mice were 8 weeks old. To minimize error from circadian rhythm, body weights were recorded each week on Fridays at 9 am. By the end of 20 weeks, the weight difference was not significant between genotypes fed a LFD (**Figure 3A**) ($p=0.26$). However, under HFD, the average weight of ACSL4 $^{L-/-}$ was 3 gram lower than that of their littermate controls. Significant weight difference developed after 20 weeks between HFD and LFD regardless of their genotypes, which indicated a diet-induced obesity. The weight difference between diets developed at week 5 ($p<0.05$) for control mice but this diet-induced weight difference was delayed until week 19 for their knockout littermates ($p<0.05$). Analysis of net weight gain during the diet period showed that mice of both genotypes fed the HFD gained more weight when compared to mice fed the LFD ($p<0.05$) (**Figure 3B**). Together these data indicate that after HFD feeding, mice developed diet-induced obesity regardless of genotypes, and the deletion of ACSL4 in liver decreased the total body mass by 3 g compared to littermate controls.

5.2 Results - Oral glucose tolerance and insulin tolerance tests were similar between genotypes

Obesity induces insulin resistance in both human and animal models. Impaired insulin response decreases glucose uptake from peripheral tissues such as adipose tissue and muscle. In liver, insulin resistance also accounts for increased gluconeogenesis which further affects lipid metabolism. In wild-type mice, obesity, altered glucose metabolism, and insulin resistance occur after a 45% HFD [63]. To test whether the insulin response differed in WT and ACSL4 $^{L-/-}$ mice, an OGTT was performed after mice were fed a HFD for 18 weeks. In our study, within the HFD group, the glucose peak at 15 minutes after gavage was slightly higher in ACSL4 $^{L-/-}$ mice compared to littermate controls, but the difference was not significant (**Figure 4A**). Calculation of the area under the curve (AUC) above the baseline glucose showed that among HFD-fed mice, the AUC of ACSL4 $^{L-/-}$ mice was higher compared to their littermate controls but not statistically different ($p=0.28$) (**Figure 4B**). Mice fed a 10% LFD showed a similar response to glucose treatment for both genotypes; however, by comparing diets, mice fed the HFD were glucose intolerant ($p^*<0.05$) compared to mice fed the LFD.

The ITT was performed one week after the OGTT. No significant differences were found between genotypes fed each diet (**Figure 5A, B**); however, with the same dose of insulin, mice fed the LFD experienced a higher rate of hypoglycemia. More than half of mice fed LFD needed to be rescued with a 20% glucose injection, whereas hypoglycemia did not occur in HFD-fed mice. Mice fed the LFD were significantly more sensitive to insulin treatment compared to mice fed the HFD. ($p^*<0.05$) To summarize, mice fed 45% HFD developed diet-induced insulin resistance (IR) after 20 weeks, but the status of IR was not different between genotypes.

5.3 Results - Liver histology by oil red O staining showed inconsistent differences of lipid content between genotypes

A liver triglyceride content of more than 10% of total liver weight, which cannot be accounted for by excessive alcohol intake or viral infection, is identified as NAFLD [67]. To detect NAFLD development in our mouse model, we used ORO staining, a technique commonly used for visualizing intracellular neutral lipids including triglycerides and cholesterol esters. Liver frozen sections were prepared without fixation, to avoid compromising the staining process. To solve this problem, we optimized a post-frozen fixing protocol by using 10% formalin to fix tissue for 30 minutes, as described in the methods section. By ORO staining, the number of lipid droplets in liver from mice fed a 45% HFD was vastly higher compared to mice fed a 10% LFD. Though different sizes of lipid droplets were observed between genotypes in the HFD-fed group, the results were not consistent in paired samples and no significant difference was found between genotypes (**Figure 6**).

5.4 Results - Liver triglyceride content

To quantify hepatic lipid content in the presence or absence of ACSL4 expression, we measured TAG mass in homogenized snap-frozen liver samples from 45% HFD fed animals after a 4 hour fast. With 7 mice for each genotype, triglyceride mass (normalized to tissue mass) was not significantly different between genotypes. **(Figure 8 and Table 3)** These data indicate that the deletion of ACSL4 in liver had no impact on triglyceride accumulation compared to littermate controls. This finding was consistent with our liver histology results.

Discussion

NAFLD was first described in 1979 by Adler and Schaffner that the disease is characterized as striking fat accumulation and increased hepatic inflammation within the liver, and it potentially leads to cirrhosis [68]. NAFLD mimics the pathogenesis of alcoholic liver disease, but it is not due to either alcohol toxicity or virus infection [68]. The term NAFLD was widely used after 1980 when Ludwig further confirmed the disease characteristics among patients with an abnormal liver function test [69]. In 2013 there were 28.8 million of American adults who suffered from NAFLD [70] and it has become a worldwide pandemic. Many studies have tried to elucidate the mechanism(s) involved in disease initiation and exacerbation. However, the mechanism(s) remain unclear.

NAFLD frequently occurs while obesity, type-2 diabetes, and hyperlipidemia are developing [71]. In fact, most NAFLD patients were moderately obese and share the many characteristics of metabolic syndrome [72]. However, these conditions also occur independently. In non-diabetic patients, the liver fat accumulation is also associated with total body mass index which is exacerbated in severe obesity [73]. Even though obesity is a major risk factor for NAFLD, non-obese individuals are also at risk of developing NAFLD [74-76].

To investigate complicated disease development, we need to incorporate interdisciplinary studies which help to dissect the question from pandemic trend in a

population to a particular mechanisms in individuals. Based upon the fact that ACSL4 is the only ACSL isoform which is over-expressed in the liver of NAFLD patients [48], we hypothesized that ACSL4, as one of the ACSL isoforms that activate—free fatty acids—for disparate lipid metabolic pathways, would be required for the development of human NAFLD. However, no research has been reported to illustrate the ACSL4 function in liver disease. Human ACSL4 and rodent ACSL4 are highly similar [15]. This enzyme similarity provides the ability to study the function of ACSL4 in a rodent model in order to mimic the human response. Thereupon, we hypothesized that deleting ACSL4 in the liver may prevent the transgenic mice from developing diet-induced NAFLD.

Our previous unpublished study with ACSL4 $^{L-/-}$ mice fed with a 45% HFD showed liver lipid content had a 50% decrease compared to wild-type controls; however, the low breeding rate of our initial mating strategy resulted in a limited number of mice therefore we only compared two ACSL4 $^{L-/-}$ mice with one C57B6 wild-type control. An improved mating strategy increased breeding rate about 2-fold, and KO mice were all matched with floxed littermate controls. The LoxP-Cre strategy was used to generate ACSL4 liver-specific knockoutby deleting exons three and four. Quantitative real time PCR showed that *Acsl4* mRNA expression was more than 94% knocked down in the ACSL4 $^{L-/-}$ liver. The diminished *Acsl4* expression did not trigger the compensatory effect on other *Acsl* isoforms. Compared to littermate controls, the protein expression of ACSL4 was completely eliminated in liver. Interestingly, total ACSL activity in liver was unchanged by the absence of ACSL4 compared to littermate controls using either arachidonic acid or palmitic acid as substrates. After a high fat diet challenge, both ACSL4 $^{L-/-}$ and littermate control mice had significant weight gain after 20 weeks compared to a sucrose-matched 10% LFD. Significant weight

loss was observed in ACSL4 $^{L-/-}$ compared to littermate controls (**Figure 3**). Further evaluations on liver lipid content showed large variations (**Figure 8**) between different individual mice but the average lipid content was similar between genotypes. Fatty liver developed in mice fed a HFD but not LFD. This result conflicted with our preliminary observation which may have been due to the limited sample size and incorrect comparisons. Serum TAG, cholesterol, and NEFA were unchanged between genotypes. Serum NEFA and total cholesterol level was significantly increased after feeding a HFD due to the large amount of saturated fat in the diet. The decreased fasting serum TAG after HFD feeding resulted in the suppression of *de novo* lipogenesis in liver. While mice fed the isocaloric LFD which contains a high amount of carbohydrates, they had an increase in *de novo* lipogenesis to compensate for the loss of fat. These data are consistent with a previous study which showed the increased carbohydrate content in the LFD induces de novo lipid synthesis and VLDL secretion in liver [77]. Overall, the absence of liver ACSL4 did not induce any alteration on the ability of reproduction, glucose/insulin responses, total ACSL activity in liver, or hepatic lipid metabolism. Only total body weight difference has been observed in the liver-specific ACSL4 knockout, but the effect is unrelated to liver lipid metabolism and NAFLD development.

Identical to other ACSL isoforms, ACSL4 also can facilitate FA activation by forming acyl-CoAs. However, chromosomal location, tissue distribution, subcellular location, enzyme activity and FA preferences for each ACSL isoform differ from one another. It is further implied that apart from FA activation, each isoform may affect the fate of lipid products in different metabolic pathways. *Acsl4*, also called *Facl4*, was first discovered in the rat in 1997 [26] and the gene was located on the X-chromosome [15]. The global

knockdown of ACSL4 in mice causes embryonic lethality of ACSL4 KO male offspring, decreases fertility and causes small litters of heterozygous female offspring when mated with C57B6/J male mice [50]. The data indicated ACSL4 is essential for fetal development, especially in male offspring due to the X-linked characteristic. In the ACSL4 liver-specific knockout mouse model, we did not observe any phenotype differences of pregnancy in female. To exclude sex bias and due to the higher possibility of having ACSL4 $^{L-/-}$ in male, we used ACSL4 $^{L-/-}$ male mice to detect liver-specific ACSL4 knockout phenotype differences. Significant decrease in total body weight was found in ACSL4 $^{L-/-}$ male mice after 20 weeks HFD challenge, compared to littermate controls (**Figure 3**). This result indicated merely removing ACSL4 from liver may reduce growth rate and weight gain, but the mechanism of how ACSL4 changes total body weight needs to be further investigated.

ACSL4 has a distinct tissue distribution [26]. In humans, *ACSL4* RNA is widely distributed in brain, heart muscle, and skeleton muscle, and reproductive organs, but it was not detected in liver [15]. A small amount of protein expression is found in human hepatocytes, whereas there is a larger amount of expression found in the cerebellum, adrenal, or testis (www.proteinatlas.org). In our mouse model, western blot showed the similar existence of abundant ACSL4 in cerebellum and adrenal glands of both KO and control mice (**Figure 2B**); however, ACSL4 in testis of both genotypes was difficult to detect (data not shown). This fact raises the question of whether ACSL4 would be up-regulated in mice after NAFLD development. ACSL4 function in human and rodents may vary after the onset of liver disease onset.

Due to differential splicing, *ACSL4* expression produces two variants, a brain-specific isoform variant 2 [24, 25] and a ubiquitous variant 1 [9]. Variant 1 has been found to

associate with the inner plasma membrane as well as in the cytosol[9]. In our project, total ACS activity was measured by using liver homogenates from ACSL4 $^{L-/-}$ and littermate controls. The removal of ACSL4 in liver did not influence enzyme specific activity when using either palmitic acid or arachidonic acid, the preferred fatty acid for ACSL4 [26]. It might because ACSL4, as a minor amount of ACSL isoform in liver, did not contribute to the activation of fatty acids. In fact, in the ACSL1 liver-specific KO model, the ACSL specific activity was 50% lower compared to control which indicated the ACSL1 is an abundant hepatic ACSL isoform [60]. Therefore, in ACSL4 $^{L-/-}$ liver, total ACSL activity is unaffected by the removal of ACSL4.

The liver, serves as the central lipid factory, and governs various lipid species production and transportation throughout the body. This process not only refers to the intake of lipoprotein particles from circulation, but also includes lipid assembly and output, and energy maintenance for liver itself. Meanwhile, this whole system is modulated under different health conditions and diet challenges. Dietary lipids and FAs released from adipose tissues comprise the lipid influx to liver. Within liver, *de novo* lipogenesis is stimulated by insulin signaling and is increased by energy surplus. Furthermore, abundant energy promotes triglyceride synthesis which can be either stored or released from liver into blood circulation as VLDL. Under energy depletion, fatty acids from either the local lipid pool or the free fatty acid derived from adipose tissue lipolysis are degraded through oxidation for energy production. Under insulin resistant state, which was also established in our mouse model (**Figure 4, 5**), enhanced circulating FAs influx and hyperinsulinemia stimulates hepatic lipid synthesis and blunts hepaticβ-oxidation. By assuming that lack of ACSL4 was protective against NAFLD, we expected to see a phenotype difference on hepatic lipid accumulation

because it is the main feature of NAFLD [45]. However, after 20 weeks 45% HFD, no difference in hepatic lipid content was found between ACSL4 $^{L-/-}$ and littermate controls (**Figure 8, Table 3**), and triglyceride levels largely differed from each individuals. Therefore, we conclude that activated FFA by ACSL4 in liver may not be required for lipid accumulation. Alternatively, ACSL4-derived products may be used in signaling molecules formation and affect the growth process of other tissues such as skeleton muscle which would require further investigation.

Conclusion and further investigations

Taken together, in liver-specific ACSL4 knockout mice, the absence of ACSL4 did not have major effects on hepatic lipid accumulation. No phenotypic difference was observed when mice were fed a high fat diet which induces impaired insulin response and glucose intolerance, and enhanced serum lipid content in both genotypes. I concluded that the ACSL4 deletion does not prevent the onset of NAFLD in mice.

Compared to hepatic ACSL4 function, neurological development and carcinogenesis research reported that ACSL4 is highly related to those diseases pathogenesis. *Drosophila*, as a model for neurological science, was widely used to investigate ACSL4 neuronal functions [78]. *Drosophila dAcsl* is an ortholog of human *ACSL3* and *ACSL4* [78]. It was also identified to localize on ER [78] which is the same localization as human ACSL4 variant 2 [23, 24]. During the formation of glia and neurons, lack of ACSL4 resulted in reduction of decapentaplegic (Dpp), one of the *Drosophila* vertebrate bone morphogenetic proteins (BMP) homologs [78]. Dpp signaling was reported to initiate neuronal differentiation and proliferation [79]. ACSL4 mutation blunts the Dpp signaling pathway and further impedes neuron development which may mimic a pathogenic process in human X-link mental retardation [78]. Synaptic growth, however, was inhibited by ACSL4 homolog dAcsl by attenuating BMP signaling [80]. Therefore, even within brain, ACSL4 has specific function in different regions. Even though ACSL4 function in brain has not been fully understood,

mounting research suggests that ACSL4-derived lipid products may have important effects on neuron growth and signaling transmission [81]. A potential assumption of neuronal ACSL4 function is membrane formation which may involve ACSL4-derived phospholipids which contain arachidonic acid [82]. Lack of ACSL4 impairs neuronal differentiation and an increased content of prostaglandin accumulate in neurons [82].

Other than neuronal development, overexpressed ACSL4 was detected in multiple cancer cell lines, including specific type of human breast cancer[48], colon cancer [52], and liver cancer [47]. It has been found to positively regulate cancer cell growth. Intracellular free arachidonic acid level is reduced by overexpressing ACSL4 and COX-2 in colon cancer and apoptosis is prevented by the excessive enzyme expression [52]. On the contrary, increasing the intracellular AA level by using triacin C to inhibit ACSL activity or by adding exogenous AA, induced apoptosis [52]. In hepatoma cells, increased ACSL4 expression has been found, and the inhibition of ACSL4 expression directly decreased cancer cell growth [47]. In this study, by adding one type of cyclic AMP (cAMP) analog – one of the second messengers in intracellular signaling pathway – ACSL4 expression is suppressed in the hepatoma cells [47]. To investigate downstream pathway of cAMP and ACSL4 interaction, the study found that p38 phosphorylation was up-regulated in tumors cells but its activity can be restricted by cAMP [47]. p38 can be stimulated by growth factors, cytokines, and it transmits intracellular signaling to nuclei by modulating gene expression [83]. By using p38 inhibitor, the study found the ACSL4 expression was blocked [47]. This result suggested that p38 was involved in the interaction of cAMP and ACSL4 expression in hepatoma cells [47].

There are several limitations of my current project which can be improved in future investigation. First, we need biomarkers to identify the development of NAFLD. Even

though increasing hepatic lipid content is the major marker of fatty liver, in our study not all mice fed with a 45% HFD established a dramatic increase of liver triglyceride which happened in both KO and littermate controls. During the progression of NAFLD, liver cells rupture and release hepatic ALT and AST into the blood stream. Hepatic ALT and AST can be detected in serum to determine disease onset. Second, significant weight loss was observed in ACSL4 $^{L-/-}$ male mice (n=10) fed a 45% HFD for 20 weeks. The current research indicated ACSL4 liver-deletion did not alter liver lipid metabolism; however, the liver-specific genetic change may affect nutritional metabolism in other tissues by releasing signaling molecules. Furthermore, the weight difference may also relate to food intake, basal metabolic rate and physical activity, and different lean/fat mass proportion. Third, different proportion of phospholipid FA species may result from the lack of ACSL4. A recent study indicated that increased phosphatidylinositol was observed along with ACSL4 overexpression which supports my conclusions [9]. I assume that removal of ACSL4 in liver will alter phospholipid metabolism even if ACSL1 is supposed to be the predominant ACSL isoform in mouse liver, because an overexpressing ACSL4 was observed to alter phospholipid formation rather than ACSL1 [9]. Fourth, in my current project, although no evidence elucidated a possible causality between hepatic ACSL4 function and NAFLD development, ACSL4 itself could be a biomarker for NAFLD onset.

A.

B.

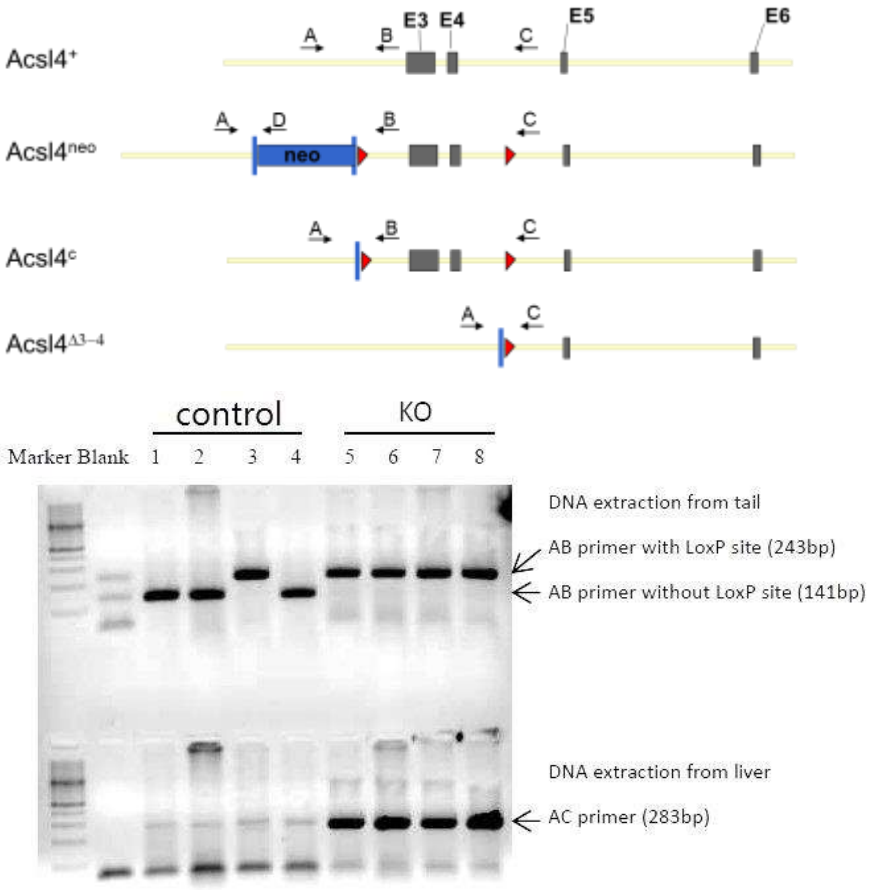

Figure1. *Acsl4* flox PCR strategies

A. By flanking LoxP sites at sides of exon 3 and 4, the targeting gene structure yielded exon 3 and 4 deletion when crossed to albumin-CRE animals. Deletion of exons 3 and 4 caused immediate translational stops from exon 2 to downstream exons which stopped ACSL4 protein expression. Neo sequence helps to screen the positive transgene. After back-crossing 10 times to C57BL/6 mice, *Acsl4* flox gene was stable in C57BL/6 background.
B. PCR amplification of loxP site and *Acsl4* deletion in liver. Heterozygous ACSL4 $^{+/-}$ female mice were interbred with Alb-cre heterozygous male mice to produce ACSL4 $^{L-/-}$ mice and littermates controls. A 243 bp band indicated loxP was inserted into *Acsl4* gene and a 141 bp band indicated normal *Acsl4* gene. A 283 bp PCR was produced only in the liver of KO mice.

A. B.

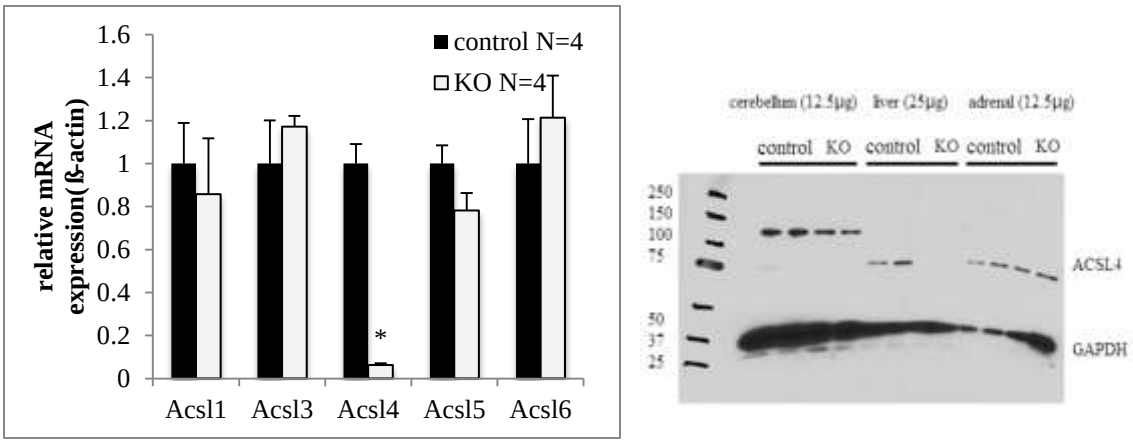

Figure2. Livers from ACSL4 $^{L-/-}$ male mice contain little *Acsl4* m RNA compared to other ACS isoforms and no ACSL4 expressed compared to littermate controls.

A. mRNA expression in liver from ACSL4 $^{L-/-}$ mice compared to liver from littermate controls. Relative gene expression of *Acsl* in ACSL4 $^{L-/-}$ mice compared to littermate controls (n = 4 for each group). Total mRNA was isolated from 20 µg liver samples by Qiagen RNeasy Mini kit, mRNA was synthesized to LFDNA for SYBR Green quantitative PCR. The 5 ACS isoforms gene expression were normalized to the endogenous control, beta-actin. *$p<0.05$ versus *Acsl4* mRNA expression in littermate controls.
B. ACSL4 protein level in the liver, cerebellum, and adrenal of ACSL4 $^{L-/-}$ mice and littermate controls mice. Homogenates made from liver, cerebellum, and adrenal tissue snap-frozen sample were subjected to SDS-PAGE by loading 12.5 µg, 25µg, and 12.5µg protein, respectively. After transfer to a polyvinylidene difluoride membrane, membranes were incubated with primary anti-ACSL4 peptide polyclonal antibody or anti-GAPDH antibody

A. B.

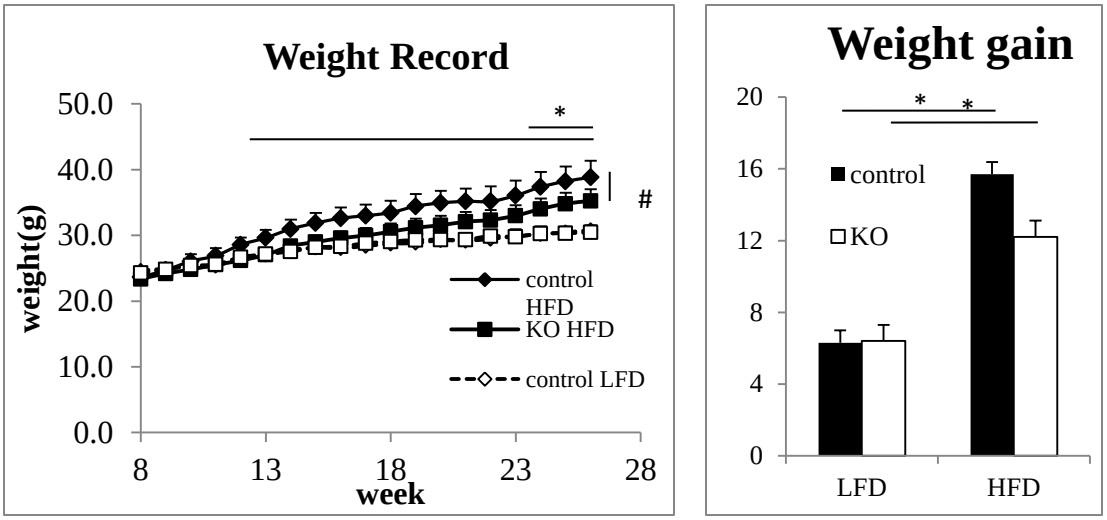

Figure3. Weight difference was observed between ACSL4 $^{L-/-}$ male mice and littermate controls at the age of 27-week fed with a 45% HFD. No difference was observed between genotypes when mice fed a 10% LFD matched for sucrose.

A. Body weight changes in ACSL4 $^{L-/-}$ male mice and littermate controls during 20 weeks fed by 45% HFD compared with 10% LFD.
* P<0.05 ACSL4 $^{L-/-}$ mice and control mice fed by HFD versus LFD (Student's t-test)
$^{\#}$ P<0.05 ACSL4 $^{L-/-}$ mice versus control mice fed a HFD at the end of the diet
B. Body weight gain at the end of 20 weeks on the appointed diets.
Data are shown as mean ±S.E. * P<0.05 versus control mice fed by LFD (Student's t-test)
(HFD control n=10, KO n=12; LFD control n=10, KO n=6)

A. B.

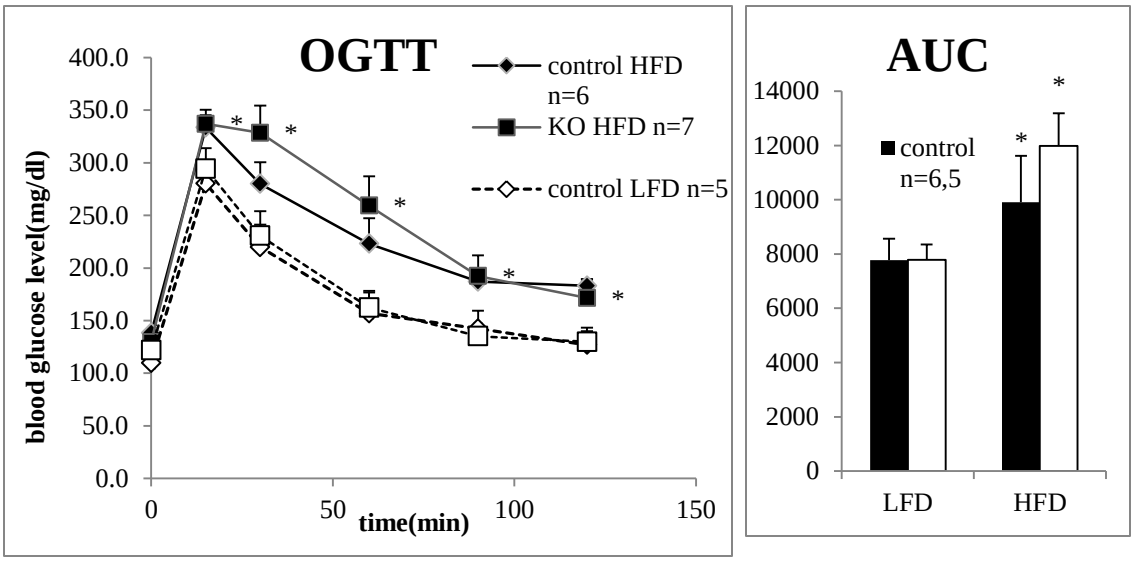

Figure4. Glucose response after a glucose oral gavage after 4 hours fast was similar of male mice of both genotypes fed a 45% HFD or a 10% LFD for 20 weeks

A. Data are shown as mean ±S.E. *p<0.05 difference between diets but not genotypes
B. Area under the curve (AUC). Data are shown as mean ±S.E. *p<0.05 difference between diets but not genotypes (n=5-7 for each group)

A. B.

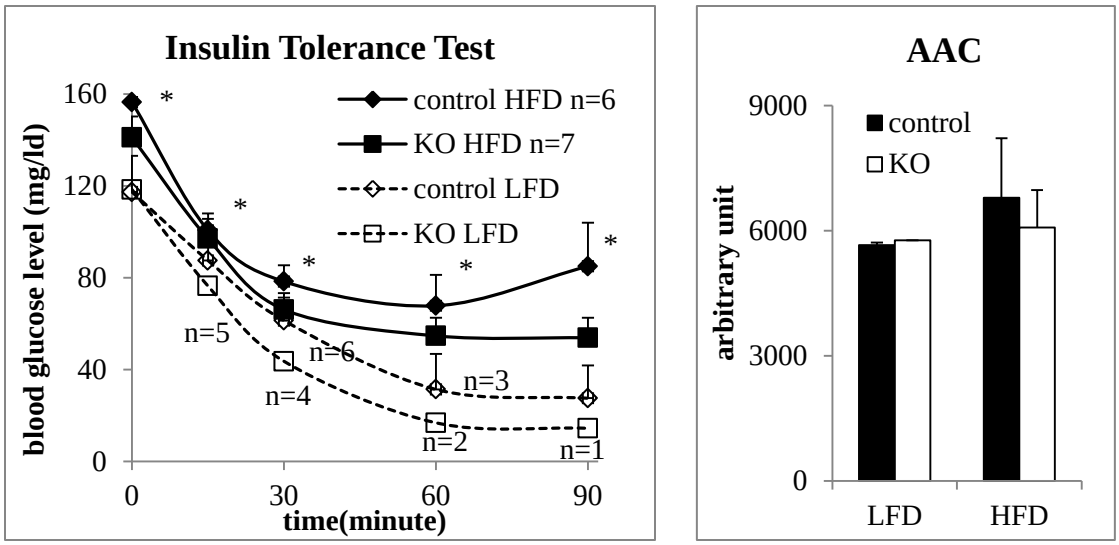

Figure5. Insulin tolerance test (ITT) after 4 hours fast on male mice fed by 45% HFD or 10% LFD for 20 weeks had no difference between genotypes.

A. Data are shown as mean ±S.E. *$p<0.05$ difference between diets but not genotypes
At the 60 minute time point, 3 control mice and 3 KO mice required rescue by glucose injection. Only 3 control mice and 1 KO mouse finished the whole experiment without rescuing.

B. Area above the curve (AAC) of mice fed by 45% HFD.
(HFD control n=6, KO n=7; LFD control n=3, KO n=1)

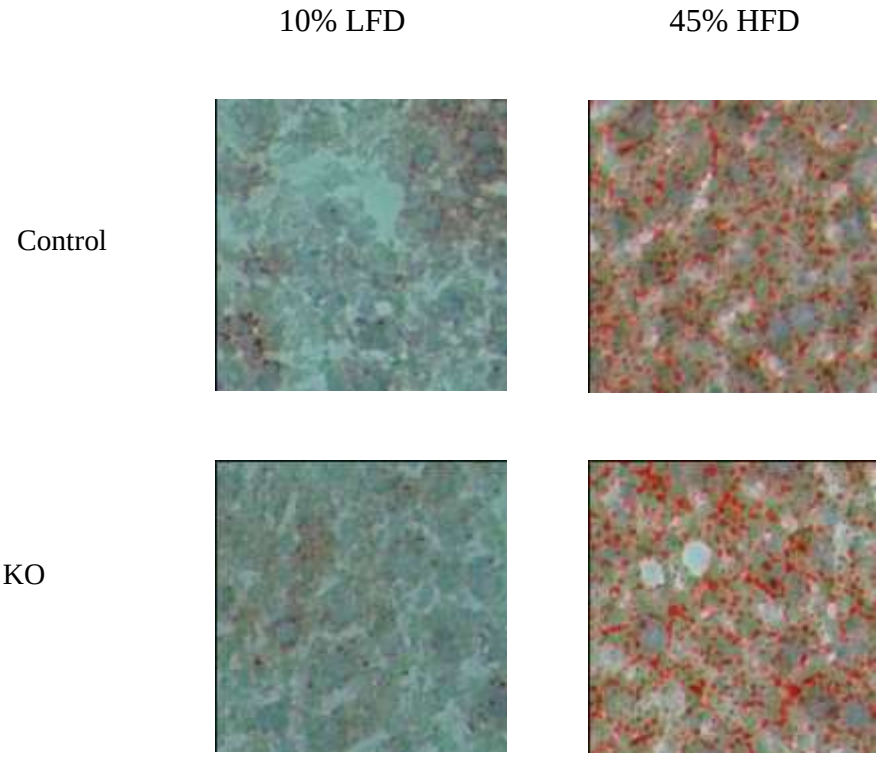

Figure6. No difference showed in liver histology with oil red O staining

Visualization of neutral lipids by ORO analysis in liver from ACSL4 $^{L-/-}$ mice and littermate controls fed with a 10% LFD or a 45% HFD for 20 weeks. Magnification is ×10 each sample; n = 3 – 4 per group.
Left two panels: Representative histology from ACSL4 $^{L-/-}$ mice fed a 10% LFD for 20 weeks. Lipid droplets were stained with ORO. Upper panel is liver from littermate control; lower panel is from KO mouse.
Right two panels: ACSL4 $^{L-/-}$ mice fed a 45% HFD for 20 weeks. Lipid droplets were stained by ORO. Upper panel is liver from littermate control; lower panel is from KO mouse.

A. B.

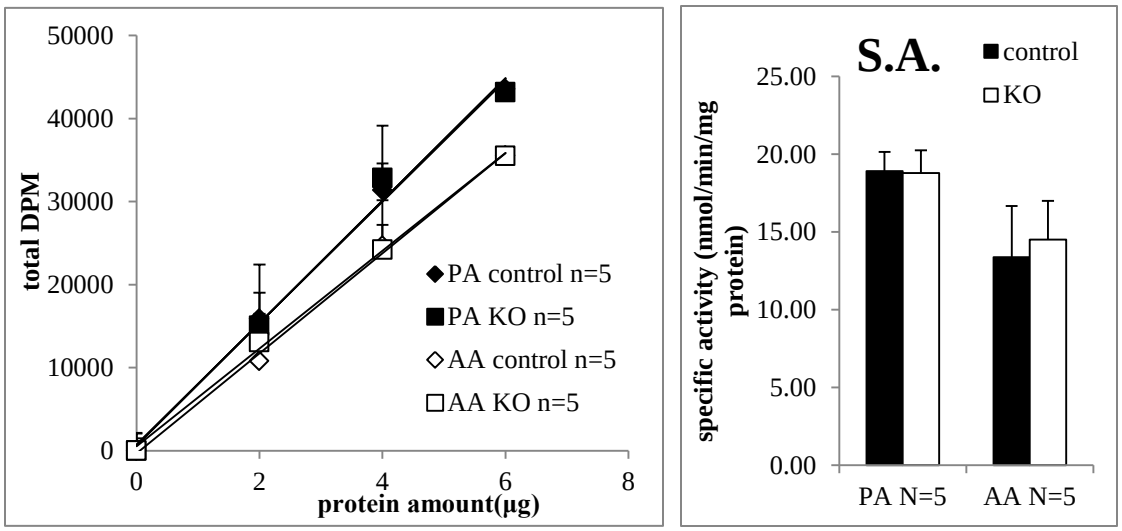

Figure7. Total ACS activity in HFD liver was unaltered by ACSL4 deletion compared to control liver samples (n=5)

A. ACSL activity in liver with [^{14}C]-palmitic acid or [^{14}C]-arachidonic acid as substrate Liver homogenates obtained from littermate controls and ACSL4 $^{L-/-}$ mice were incubated with 50uM labeled fatty acid and reaction reagent for 10 minutes at room temperature. Data are shown as mean ±S.E.

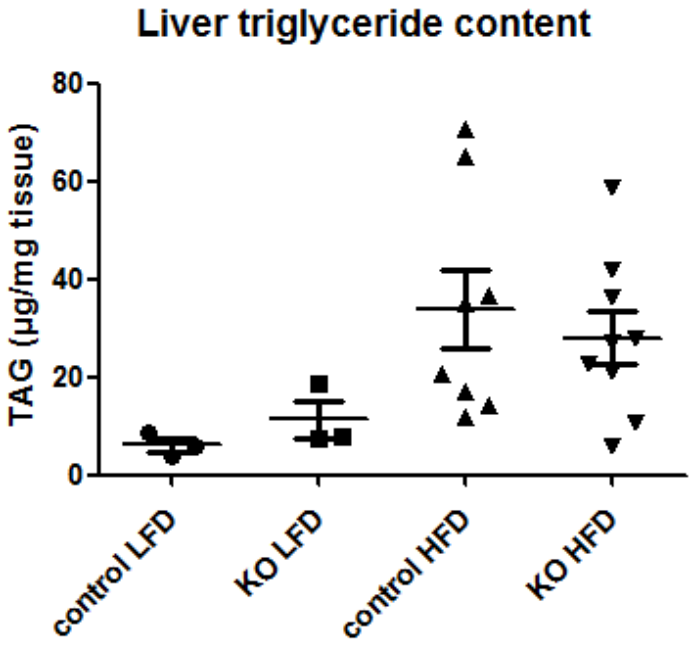

Figure8. HFD-fed mice had higher hepatic TAG content compared to LFD-fed but no difference was observed between genotypes

Control HFD n=8; KO HFD n=9; control LFD n=3; KO LFD n=3

A.

Primer	Name	Sequence
A	ACSL4-F1	CAGTCTTTGGCTGTAAATTGACTATGTGC
B	ACSL4-R1	TGTACCAGTTGCTTGGGAGGAGTACA
C	ACSL4-RSeq4	ACTTGCCAACCAGAAACATGCATAC
D	PGKPR-R1	TGCCTTGGGAAAAGCGCCTC

B.

PCR product sizes (bp)			
Allele	A-B	A-D	A-C
+	141	-	-
neo	-	243	-
c	243	-	-
Δ3-4	-	-	283

Table 1. Primer sequences and product sizes

A. Primers were designed to investigate LoxP insertion sites and *Acsl4* deletion.
B. PCR product sizes. Liver samples PCR yielded a 283 bp band with A/C primers which indicate *Acsl4* exon 3 and 4 were excised from liver (knockout mice only). Tail samples PCR produced a 243 bp band with A/B primers which means existed loxP sites and a 141 bp band with A/B primers without loxP insertion.

A. Original mating strategy

♂\♀	X^{+}	X^{-}
X^{+}	X^{+} X^{+}	X^{+} X^{-}
Y	X^{+} Y	X^{-} Y

B. Developing homozygous ACSL4 $^{floxed/floxed}$ female

♂\♀	X^{+}	X^{-}
X^{-}	X^{+} X^{-}	X^{-} X^{-}
Y	X^{+} Y	X^{-} Y

C. Current mating strategy

♂\♀	X^{-}	X^{-}
X^{+}	X^{-} X	X^{-} X
Y	X^{-} Y	X^{-} Y

Table 2 Breeding strategies of ACSL4 $^{L-/-}$ mice

A. Originally, heterozygous Acsl4 $^{+/floxed}$ female mice were interbred with heterozygous Alb-Cre male mice to produce ACSL4 $^{L-/-}$ mice with a low rate of 12.5%.
B. To improve our breeding strategy, homozygous Acsl4 $^{floxed/floxed}$ female mice was generated by crossed heterozygous Acsl4 $^{+/floxed}$ female mice with ACSL4 ^{floxed} male mice.
C. With homozygous Acsl4$^{floxed/floxed}$ female mice, new breeding strategy provide 25% generation of ACSL4 $^{L-/-}$ male mice when mating with heterozygous Alb-Cre male mice.

Table3. Lipid metabolites in serum and liver

	10% LFD		45% HFD	
Serum	control (n=3)	KO (n=3)	control (n=9)	KO (n=8)
TAG (mg/dL)	56 ±7.3	51.5 ±4.7	37 ±5.3 *	34 ±2.1 #
NEFA (mEq/L)	0.26 ±0.02	0.37 ±0.05	0.54 ±0.04 *	0.57 ±0.02
Total cholesterol (mg/dL)	90 ±6.7	104 ±9.6	144 ±8.6 *	134 ±9.1#
Liver				
TAG (μg/mg tissue)	6.2 ±1.3	11.3 ±3.7	34 ±8.1 *	28 ±5.3 #

Table 3 Liver triglyceride and serum lipid metabolites did not altered in ACSL4 $^{L-/-}$ male mice and controls after 4 hours fast

Serum collected from mice after 4 hour fast. Lipid metabolites were measured by enzymatic kits. Data showed the mean ±S.E.
Liver triglyceride was extracted by a modified Folch method with lysis buffer. TAG mass in quantitative amount of liver tissue was measured enzymatically. Data are shown as mean ±S.E.
* P<0.05 versus control mice fed by LFD (Student's t-test) $^{\#}$P<0.05 versus KO mice fed by LFD

REFERENCES

[1] Iqbal J, Hussain MM. Intestinal lipid absorption. American journal of physiology Endocrinology and metabolism 2009;296:E1183-94.

[2] Nguyen P, Leray V, Diez M, Serisier S, Le Bloc'h J, Siliart B, et al. Liver lipid metabolism. Journal of animal physiology and animal nutrition 2008;92:272-83.

[3] Julius U. Influence of plasma free fatty acids on lipoprotein synthesis and diabetic dyslipidemia. Experimental and clinical endocrinology & diabetes : official journal, German Society of Endocrinology [and] German Diabetes Association 2003;111:246-50.

[4] Adeli K, Taghibiglou C, Van Iderstine SC, Lewis GF. Mechanisms of hepatic very low-density lipoprotein overproduction in insulin resistance. Trends in cardiovascular medicine 2001;11:170-6.

[5] Wiegman CH, Bandsma RH, Ouwens M, van der Sluijs FH, Havinga R, Boer T, et al. Hepatic VLDL production in ob/ob mice is not stimulated by massive de novo lipogenesis but is less sensitive to the suppressive effects of insulin. Diabetes 2003;52:1081-9.

[6] Andreo U, Guo L, Chirieac DV, Tuyama AC, Montenont E, Brodsky JL, et al. Insulin-stimulated degradation of apolipoprotein B100: roles of class II phosphatidylinositol-3-kinase and autophagy. PloS one 2013;8:e57590.

[7] Grefhorst A, Parks EJ. Reduced insulin-mediated inhibition of VLDL secretion upon pharmacological activation of the liver X receptor in mice. Journal of lipid research 2009;50:1374-83.

[8] Soupene E, Kuypers FA. Multiple erythroid isoforms of human long-chain acyl-CoA synthetases are produced by switch of the fatty acid gate domains. BMC molecular biology 2006;7:21.

[9] Kuch EM, Vellaramkalayil R, Zhang I, Lehnen D, Brugger B, Stremmel W, et al. Differentially localized acyl-CoA synthetase 4 isoenzymes mediate the metabolic channeling of fatty acids towards phosphatidylinositol. Biochimica et biophysica acta 2013;1841:227-39.

[10] Tomoda H, Igarashi K, Cyong JC, Omura S. Evidence for an essential role of long chain acyl-CoA synthetase in animal cell proliferation. Inhibition of long chain acyl-CoA synthetase by triacsins caused inhibition of Raji cell proliferation. The Journal of biological chemistry 1991;266:4214-9.

[11] Van Horn CG, Caviglia JM, Li LO, Wang S, Granger DA, Coleman RA. Characterization of recombinant long-chain rat acyl-CoA synthetase isoforms 3 and 6: identification of a novel variant of isoform 6. Biochemistry 2005;44:1635-42.

[12] Askari B, Kanter JE, Sherrid AM, Golej DL, Bender AT, Liu J, et al. Rosiglitazone inhibits acyl-CoA synthetase activity and fatty acid partitioning to diacylglycerol and triacylglycerol via a peroxisome proliferator-activated receptor-gamma-independent mechanism in human arterial smooth muscle cells and macrophages. Diabetes 2007;56:1143-52.

[13] Lewin TM, Kim JH, Granger DA, Vance JE, Coleman RA. Acyl-CoA synthetase isoforms 1, 4, and 5 are present in different subcellular membranes in rat liver and can be inhibited independently. The Journal of biological chemistry 2001;276:24674-9.

[14] Soupene E, Kuypers FA. Mammalian long-chain acyl-CoA synthetases. Experimental biology and medicine 2008;233:507-21.

[15] Piccini M, Vitelli F, Bruttini M, Pober BR, Jonsson JJ, Villanova M, et al. FACL4, a new gene encoding long-chain acyl-CoA synthetase 4, is deleted in a family with Alport syndrome, elliptocytosis, and mental retardation. Genomics 1998;47:350-8.

[16] Mallonee DH, Adams JL, Hylemon PB. The bile acid-inducible baiB gene from Eubacterium sp. strain VPI 12708 encodes a bile acid-coenzyme A ligase. Journal of bacteriology 1992;174:2065-71.

[17] Smith DJ, Burnham MK, Edwards J, Earl AJ, Turner G. Cloning and heterologous expression of the penicillin biosynthetic gene cluster from penicillum chrysogenum. Bio/technology 1990;8:39-41.

[18] Toh H. Sequence analysis of firefly luciferase family reveals a conservative sequence motif. Protein sequences & data analysis 1991;4:111-7.

[19] Turgay K, Krause M, Marahiel MA. Four homologous domains in the primary structure of GrsB are related to domains in a superfamily of adenylate-forming enzymes. Molecular microbiology 1992;6:529-46.

[20] Vares G, Uehara Y, Ono T, Nakajima T, Wang B, Taki K, et al. Transcription factor-recognition sequences potentially involved in modulation of gene expression after exposure to low-dose-rate gamma-rays in the mouse liver. Journal of radiation research 2011;52:249-56.

[21] Sepulveda JL, Vlahopoulos S, Iyer D, Belaguli N, Schwartz RJ. Combinatorial expression of GATA4, Nkx2-5, and serum response factor directs early cardiac gene activity. The Journal of biological chemistry 2002;277:25775-82.

[22] Hilger-Eversheim K, Moser M, Schorle H, Buettner R. Regulatory roles of AP-2 transcription factors in vertebrate development, apoptosis and cell-cycle control. Gene 2000;260:1-12.

[23] Nakai K, Horton P. PSORT: a program for detecting sorting signals in proteins and predicting their subcellular localization. Trends in biochemical sciences 1999;24:34-6.

[24] Meloni I, Muscettola M, Raynaud M, Longo I, Bruttini M, Moizard MP, et al. FACL4, encoding fatty acid-CoA ligase 4, is mutated in nonspecific X-linked mental retardation. Nature genetics 2002;30:436-40.

[25] Mashek DG, Bornfeldt KE, Coleman RA, Berger J, Bernlohr DA, Black P, et al. Revised nomenclature for the mammalian long-chain acyl-CoA synthetase gene family. Journal of lipid research 2004;45:1958-61.

[26] Kang MJ, Fujino T, Sasano H, Minekura H, Yabuki N, Nagura H, et al. A novel arachidonate-preferring acyl-CoA synthetase is present in steroidogenic cells of the rat adrenal, ovary, and testis. Proceedings of the National Academy of Sciences of the United States of America 1997;94:2880-4.

[27] Cao Y, Traer E, Zimmerman GA, McIntyre TM, Prescott SM. Cloning, expression, and chromosomal localization of human long-chain fatty acid-CoA ligase 4 (FACL4). Genomics 1998;49:327-30.

[28] Cao Y, Pearman AT, Zimmerman GA, McIntyre TM, Prescott SM. Intracellular unesterified arachidonic acid signals apoptosis. Proceedings of the National Academy of Sciences of the United States of America 2000;97:11280-5.

[29] Neufeld EJ, Bross TE, Majerus PW. A mutant HSDM1C1 fibrosarcoma line selected for defective eicosanoid precursor uptake lacks arachidonate-specific acyl-CoA synthetase. The Journal of biological chemistry 1984;259:1986-92.

[30] Wilson DB, Prescott SM, Majerus PW. Discovery of an arachidonoyl coenzyme A synthetase in human platelets. The Journal of biological chemistry 1982;257:3510-5.

[31] Getz GS, Bartley W, Stripe F, Notton BM, Renshaw A, Robinson DS. The lipid composition of rat-liver cell sap. The Biochemical journal 1961;81:214-20.

[32] Fex G. Metabolism of phosphatidyl choline, phosphatidyl ethanolamine and sphingomyelin in regenerating rat liver. Biochimica et biophysica acta 1971;231:161-9.

[33] Dennis EA, Rhee SG, Billah MM, Hannun YA. Role of phospholipase in generating lipid second messengers in signal transduction. FASEB journal : official publication of the Federation of American Societies for Experimental Biology 1991;5:2068-77.

[34] Natarajan R, Nadler JL. Lipid inflammatory mediators in diabetic vascular disease. Arteriosclerosis, thrombosis, and vascular biology 2004;24:1542-8.

[35] Kroetz DL, Zeldin DC. Cytochrome P450 pathways of arachidonic acid metabolism. Current opinion in lipidology 2002;13:273-83.

[36] Smyth EM, Grosser T, Wang M, Yu Y, FitzGerald GA. Prostanoids in health and disease. Journal of lipid research 2009;50 Suppl:S423-8.

[37] Wang X, Stocco DM. Cyclic AMP and arachidonic acid: a tale of two pathways. Molecular and cellular endocrinology 1999;158:7-12.

[38] Cipollone F, Rocca B, Patrono C. Cyclooxygenase-2 expression and inhibition in atherothrombosis. Arteriosclerosis, thrombosis, and vascular biology 2004;24:246-55.

[39] Klett EL, Chen S, Edin ML, Li LO, Ilkayeva O, Zeldin DC, et al. Diminished acyl-CoA synthetase isoform 4 activity in INS 832/13 cells reduces cellular epoxyeicosatrienoic acid levels and results in impaired glucose-stimulated insulin secretion. The Journal of biological chemistry 2013;288:21618-29.

[40] Cao Y, Murphy KJ, McIntyre TM, Zimmerman GA, Prescott SM. Expression of fatty acid-CoA ligase 4 during development and in brain. FEBS letters 2000;467:263-7.

[41] Seppala-Lindroos A, Vehkavaara S, Hakkinen AM, Goto T, Westerbacka J, Sovijarvi A, et al. Fat accumulation in the liver is associated with defects in insulin suppression of glucose production and serum free fatty acids independent of obesity in normal men. The Journal of clinical endocrinology and metabolism 2002;87:3023-8.

[42] Adiels M, Taskinen MR, Packard C, Caslake MJ, Soro-Paavonen A, Westerbacka J, et al. Overproduction of large VLDL particles is driven by increased liver fat content in man. Diabetologia 2006;49:755-65.

[43] Ryysy L, Hakkinen AM, Goto T, Vehkavaara S, Westerbacka J, Halavaara J, et al. Hepatic fat content and insulin action on free fatty acids and glucose metabolism rather than insulin absorption are associated with insulin requirements during insulin therapy in type 2 diabetic patients. Diabetes 2000;49:749-58.

[44] Makkonen J, Westerbacka J, Kolak M, Sutinen J, Corner A, Hamsten A, et al. Increased expression of the macrophage markers and of 11beta-HSD-1 in subcutaneous adipose tissue, but not in cultured monocyte-derived macrophages, is associated with liver fat in human obesity. International journal of obesity 2007;31:1617-25.

[45] Kleiner DE, Brunt EM, Van Natta M, Behling C, Contos MJ, Cummings OW, et al. Design and validation of a histological scoring system for nonalcoholic fatty liver disease. Hepatology 2005;41:1313-21.

[46] Neuschwander-Tetri BA, Caldwell SH. Nonalcoholic steatohepatitis: summary of an AASLD Single Topic Conference. Hepatology 2003;37:1202-19.

[47] Liang YC, Wu CH, Chu JS, Wang CK, Hung LF, Wang YJ, et al. Involvement of fatty

acid-CoA ligase 4 in hepatocellular carcinoma growth: roles of cyclic AMP and p38 mitogen-activated protein kinase. World journal of gastroenterology : WJG 2005;11:2557-63.

[48] Wu X, Li Y, Wang J, Wen X, Marcus MT, Daniels G, et al. Long chain fatty Acyl-CoA synthetase 4 is a biomarker for and mediator of hormone resistance in human breast cancer. PloS one 2013;8:e77060.

[49] Maloberti PM, Duarte AB, Orlando UD, Pasqualini ME, Solano AR, Lopez-Otin C, et al. Functional interaction between acyl-CoA synthetase 4, lipooxygenases and cyclooxygenase-2 in the aggressive phenotype of breast cancer cells. PloS one 2010;5:e15540.

[50] Cho YY, Kang MJ, Sone H, Suzuki T, Abe M, Igarashi M, et al. Abnormal uterus with polycysts, accumulation of uterine prostaglandins, and reduced fertility in mice heterozygous for acyl-CoA synthetase 4 deficiency. Biochemical and biophysical research communications 2001;284:993-7.

[51] Kudo T, Tamagawa T, Kawashima M, Mito N, Shibata S. Attenuating effect of clock mutation on triglyceride contents in the ICR mouse liver under a high-fat diet. Journal of biological rhythms 2007;22:312-23.

[52] Cao Y, Dave KB, Doan TP, Prescott SM. Fatty acid CoA ligase 4 is up-regulated in colon adenocarcinoma. Cancer research 2001;61:8429-34.

[53] Sung YK, Hwang SY, Park MK, Bae HI, Kim WH, Kim JC, et al. Fatty acid-CoA ligase 4 is overexpressed in human hepatocellular carcinoma. Cancer science 2003;94:421-4.

[54] Kotronen A, Yki-Jarvinen H, Aminoff A, Bergholm R, Pietilainen KH, Westerbacka J, et al. Genetic variation in the ADIPOR2 gene is associated with liver fat content and its surrogate markers in three independent cohorts. European journal of endocrinology / European Federation of Endocrine Societies 2009;160:593-602.

[55] Watkins PA, Maiguel D, Jia Z, Pevsner J. Evidence for 26 distinct acyl-coenzyme A synthetase genes in the human genome. Journal of lipid research 2007;48:2736-50.

[56] Postic C, Magnuson MA. DNA excision in liver by an albumin-Cre transgene occurs progressively with age. Genesis 2000;26:149-50.

[57] Folch J, Lees M, Sloane Stanley GH. A simple method for the isolation and purification of total lipides from animal tissues. The Journal of biological chemistry 1957;226:497-509.

[58] Samuel VT, Liu ZX, Qu X, Elder BD, Bilz S, Befroy D, et al. Mechanism of hepatic insulin resistance in non-alcoholic fatty liver disease. The Journal of biological chemistry 2004;279:32345-53.

[59] Li LO, Mashek DG, An J, Doughman SD, Newgard CB, Coleman RA. Overexpression of rat long chain acyl-coa synthetase 1 alters fatty acid metabolism in rat primary hepatocytes. The Journal of biological chemistry 2006;281:37246-55.

[60] Li LO, Ellis JM, Paich HA, Wang S, Gong N, Altshuller G, et al. Liver-specific loss of long chain acyl-CoA synthetase-1 decreases triacylglycerol synthesis and beta-oxidation and alters phospholipid fatty acid composition. The Journal of biological chemistry 2009;284:27816-26.

[61] Westerbacka J, Kolak M, Kiviluoto T, Arkkila P, Siren J, Hamsten A, et al. Genes involved in fatty acid partitioning and binding, lipolysis, monocyte/macrophage recruitment, and inflammation are overexpressed in the human fatty liver of insulin-resistant subjects. Diabetes 2007;56:2759-65.

[62] Marchesini G, Brizi M, Bianchi G, Tomassetti S, Bugianesi E, Lenzi M, et al. Nonalcoholic fatty liver disease: a feature of the metabolic syndrome. Diabetes 2001;50:1844-50.

[63] DeAngelis RA, Markiewski MM, Taub R, Lambris JD. A high-fat diet impairs liver regeneration in C57BL/6 mice through overexpression of the NF-kappaB inhibitor, IkappaBalpha. Hepatology 2005;42:1148-57.

[64] Black BL, Croom J, Eisen EJ, Petro AE, Edwards CL, Surwit RS. Differential effects of fat and sucrose on body composition in A/J and C57BL/6 mice. Metabolism: clinical and experimental 1998;47:1354-9.

[65] J. F. C57BL/6NHsd male mice started on high-fat diets at three, six, or nine weeks of age attain similar obesity phenotypes FASEB J 2010;554.6.

[66] Duval C, Thissen U, Keshtkar S, Accart B, Stienstra R, Boekschoten MV, et al. Adipose tissue dysfunction signals progression of hepatic steatosis towards nonalcoholic steatohepatitis in C57BL/6 mice. Diabetes 2010;59:3181-91.

[67] Deivanayagam S, Mohammed BS, Vitola BE, Naguib GH, Keshen TH, Kirk EP, et al. Nonalcoholic fatty liver disease is associated with hepatic and skeletal muscle insulin resistance in overweight adolescents. The American journal of clinical nutrition 2008;88:257-62.

[68] Adler M, Schaffner F. Fatty liver hepatitis and cirrhosis in obese patients. The American journal of medicine 1979;67:811-6.

[69] Ludwig J, Viggiano TR, McGill DB, Oh BJ. Nonalcoholic steatohepatitis: Mayo Clinic experiences with a hitherto unnamed disease. Mayo Clinic proceedings 1980;55:434-8.

[70] Lazo M, Hernaez R, Eberhardt MS, Bonekamp S, Kamel I, Guallar E, et al. Prevalence of nonalcoholic fatty liver disease in the United States: the Third National Health and

Nutrition Examination Survey, 1988-1994. American journal of epidemiology 2013;178:38-45.

[71] Angulo P. Nonalcoholic fatty liver disease. The New England journal of medicine 2002;346:1221-31.

[72] Marchesini G, Marzocchi R, Agostini F, Bugianesi E. Nonalcoholic fatty liver disease and the metabolic syndrome. Current opinion in lipidology 2005;16:421-7.

[73] Gastaldelli A, Cusi K, Pettiti M, Hardies J, Miyazaki Y, Berria R, et al. Relationship between hepatic/visceral fat and hepatic insulin resistance in nondiabetic and type 2 diabetic subjects. Gastroenterology 2007;133:496-506.

[74] Bellentani S, Saccoccio G, Masutti F, Croce LS, Brandi G, Sasso F, et al. Prevalence of and risk factors for hepatic steatosis in Northern Italy. Annals of internal medicine 2000;132:112-7.

[75] Das K, Das K, Mukherjee PS, Ghosh A, Ghosh S, Mridha AR, et al. Nonobese population in a developing country has a high prevalence of nonalcoholic fatty liver and significant liver disease. Hepatology 2010;51:1593-602.

[76] Oresic M, Hyotylainen T, Kotronen A, Gopalacharyulu P, Nygren H, Arola J, et al. Prediction of non-alcoholic fatty-liver disease and liver fat content by serum molecular lipids. Diabetologia 2013;56:2266-74.

[77] Schwarz JM, Linfoot P, Dare D, Aghajanian K. Hepatic de novo lipogenesis in normoinsulinemic and hyperinsulinemic subjects consuming high-fat, low-carbohydrate and low-fat, high-carbohydrate isoenergetic diets. The American journal of clinical nutrition 2003;77:43-50.

[78] Zhang Y, Chen D, Wang Z. Analyses of mental dysfunction-related ACSl4 in Drosophila reveal its requirement for Dpp/BMP production and visual wiring in the brain. Human molecular genetics 2009;18:3894-905.

[79] Takaesu NT, Hyman-Walsh C, Ye Y, Wisotzkey RG, Stinchfield MJ, O'Connor M B, et al. dSno facilitates baboon signaling in the Drosophila brain by switching the affinity of Medea away from Mad and toward dSmad2. Genetics 2006;174:1299-313.

[80] Liu Z, Huang Y, Hu W, Huang S, Wang Q, Han J, et al. dAcsl, the Drosophila Ortholog of Acyl-CoA Synthetase Long-Chain Family Member 3 and 4, Inhibits Synapse Growth by Attenuating Bone Morphogenetic Protein Signaling via Endocytic Recycling. The Journal of neuroscience : the official journal of the Society for Neuroscience 2014;34:2785-96.

[81] Najmabadi H, Hu H, Garshasbi M, Zemojtel T, Abedini SS, Chen W, et al. Deep sequencing reveals 50 novel genes for recessive cognitive disorders. Nature 2011;478:57-63.

[82] Cho YY. A novel role of brain-type ACS4 isotype in neuronal differentiation. Biochemical and biophysical research communications 2012;419:505-10.

[83] Ono K, Han J. The p38 signal transduction pathway: activation and function. Cellular signalling 2000;12:1-13.